Basic Zinc Cubane-1,4-Dicarboxylate: A new MOF-5 Analogous with High Porosity and Robust Dynamics

Dávid Földes[1,2], Éva Kováts[1], Gábor Bortel[1], Szilvia Klébert[3], Emma Jakab[3] and Sándor Pekker[1,4]*

[1]Institute for Solid State Physics and Optics, Wigner Research Centre for Physics, Hungarian Academy of Sciences, H-1525 Budapest, P.O. Box 49, Hungary

[2]Doctoral School on Materials Sciences and Technologies, Óbuda University, Bécsi út 96/b, H-1034 Budapest, Hungary

[3]Institute of Materials and Environmental Chemistry, Research Centre for Natural Sciences, Hungarian Academy of Sciences, H-1519 Budapest, P.O. Box 286, Hungary

[4]Faculty of Light Industry and Environmental Engineering, Óbuda University, Doberdó út 6, H-1034 Budapest, Hungary

KEYWORDS cubane, MOF, robust dynamics, crystal structure

ABSTRACT

A new metal-organic framework, basic zinc cubane-1,4-dicarboxylate, (**1**) was synthesized. **1** is a cubic framework of the same underlying topology, as basic zinc terephthalate, MOF-5, with similar lattice parameters, unique dynamics and competitive adsorption properties. It has a high-symmetry space group, $Pm\bar{3}m$ with a lattice parameter of 12.776 Å, as determined by X-ray diffraction at 100 K. The structure consists of a random distribution of two perpendicular basic zinc carboxylate nodes and axially disordered cubylene spacers, so the observed high-symmetry structure is an average of several lower-symmetry unit cells. The binary orientational disorder of the nodes has significant influence on the uniaxial rotation of the edges, realizing a previous idea of robust dynamics[1]. The structural and dynamical differences of **1** and MOF-5 are based on the local symmetry and the electronic structure of the organic components: *i)* the lack of conjugation in cubane-1,4-dicarboxylate does not fix the orientation of the nodes; and *ii)* the incomplete match of the cubylene (rotor) and dicarboxylate (stator) units facilitates the rotation of the cubylene units even at 100 K. The calculated rotation barrier is unusually low, and it depends on the orientation of the adjacent carboxylate units. The crystals of **1** can be activated either at elevated temperature in vacuum or at ambient conditions by solvent exchange. The high surface area (3160 m^2g^{-1}) and the high capacity of hydrogen uptake promise future practical applications.

INTRODUCTION

Metal-organic frameworks (MOFs) are high-porosity crystalline materials. Due to their unique structures and properties, MOFs became the most intensively studied solids of the beginning of the 21st century[2]. Based on the chemical composition, they are considered as coordination polymers of transition metals or rare earths, but the robust character of the coordination bonds

and the common structure and properties justify the distinguished nomenclature[3]. Although several related structures were known previously[4,5], an explosion-like development of this family of materials was initiated by the pioneering works of Yaghi and coworkers[6], who prepared the prototype of MOFs, the cubic framework of basic zinc terephthalate, (MOF-5) and invented a series of related structures with finely tuned lattice parameters, the so-called IRMOF series[7]. This series consists of the same basic Zn-carboxylate nodes or secondary building units (SBUs) as widely known. The SBUs are connected by various organic spacers. The development of the first few members was followed by intensive studies and exceptionally large number of new materials were produced and characterized within a couple of years[2]. The large-scale production of the new MOFs with promising properties was also developed[8,9]. Diverse functional groups were applied in MOFs: besides the most frequent carboxylates[6], also imidazolates[10], phosphonates[11], and triazine derivatives[12] were built up in the structures. The major importance of MOFs is based on the uniform pore-structure of extremely high free volume, which can be a host for a great variety of guest molecules[2,9,13-16]. The highly selective supramolecular interactions with various guest molecules can be applied to separate mixtures of small molecules[13,9]. Guest-guest and host-guest type reactions can be performed with chemically reactive guest molecules. Polymerization inside the pores[17] is an example of the first type, while catalytic reactions[18] and post-synthetics modifications[19] represent the second type. In addition to the supramolecular reactions, the hybrid nature of the metal-containing nodes and organic edges may result in interesting optical and magnetic properties[20-22]. Besides the structure, the dynamics of some MOFs may be remarkable. Stoddart, Yaghi and their coworkers[1] pointed out the importance of rotating spacer units for the application of MOFs as molecular machines. They drew the attention to the so-called robust dynamics, *i.e.*, to stable frames containing easily

rotating units and they also suggested a few possible candidates of such systems. In MOFs of primitive cubic (pcu) topology, the nodes form a robust stator system. In the majority of structures, the spacers are rigid groups with aromatic character and the conjugation with the nodes prevents their rotation. The jump-rotation of the *p*-phenylene spacer (MOF-5) was demonstrated at elevated temperatures, corresponding to a high barrier[23,24]. The insertion of ethynylene units (-C≡C-) between the phenylene rings and the carboxylic groups results in the formation of a nearly barrierless rotor[23]. Note, that some MOF structures with ethynylene units have exceptional properties; for example, NU-100 has the highest reported gravimetric H_2 uptake capacity (16,4 m/m% at 77 K and 70 bars)[25] and NU-110 has the highest reported surface area (SBET = 7140 m^2g^{-1})[26]. The dynamics of the bis-ethynyl derivatives resembles[27] the previously developed supramolecular rotor-stator crystals of fullerene-cubane[28]. More complex motion can be achieved by functionalization of the rotor units with macrocycles[29,30]. The asymmetric rotors may be the basic units of future molecular machines.

The modular structure of the SBUs and the spacers[31] comprise so many possible MOFs that simple frameworks, like the cubane derivative discussed below, have been neglected despite the systematic studies of the last decade. Cubane-dicarboxylate linker has already been used[32], but the formed 2D polymer with "paddlewheel" $Zn_2(CO_2)_4$ SBUs, called MOF-104, has not been studied in detail. A similar low-symmetry ruthenium[33] complex was also reported with cubane-1,4-dicarboxylate linkers and paddlewheel-like $Ru_2(CO_2)_4$ SBUs. However, no higher symmetry, 3D MOF structures were reported with cubane-1,4-dicarboxylate linkers. In this paper, we describe the formation, structure and properties of a MOF-5 analogue framework, (**1**) basic zinc cubane-1,4-dicarboxylate. The underlying topologies of **1** and MOF-5 are equally pcu, but their

space groups and lattice parameters are different: $Pm\bar{3}m$, $a \approx 12.8$ Å and $Fm\bar{3}m$, $a \approx 25.6$ Å, respectively.

The motivation of this work is based on the comparison of the molecular structures of terephthalic acid and cubane-1,4-dicarboxylic acid, the organic precursors of MOF-5 and the present framework, respectively. The spatial extensions of the two molecules are almost the same along the main axes: the difference of the distances of the carboxylic groups is only 10 pm. The similar sizes of the two molecules and the axial location of the two coordinating carboxylate groups suggest the possible formation of a MOF-5 analogue framework with cubane-1,4-dicarboxylate edges. The similar dimensions of the expected structure promise future supramolecular applications. On the other hand, the different chemical nature of the alicyclic cubylene spacer may give rise to different supramolecular interactions of the new framework, further enriching the remarkable adsorption properties of the IRMOF family. In addition to the supramolecular characteristics, the dynamics of cubane-dicarboxylate derivative **1** may also be significantly different from that of MOF-5. Framework **1**, the cubane-1,4-dicarboxylate analogous of MOF-5 is a promising structure of robust dynamics[1]. The lack of conjugation in alicyclic dicarboxylate ion of **1** may facilitate the uniaxial rotation of the cubylene units. The activation energy of the rotation, calculated in DFT level, is much less than that of MOF-5 and depends on the orientations of the adjacent SBUs. The new framework, discussed below, demonstrates that cubane-1,4-dicarboxylate may be the organic linker of a new family of MOFs with promising supramolecular and dynamical properties.

EXPERIMENTAL AND THEORETICAL METHODS

Synthesis. To take advantage of the similar molecular structures of terephthalate and cubane-1,4-dicarboxylate, we adapted the synthetic methods, worked out previously for MOF-5. High-quality single crystals of basic zinc cubane-1,4-dicarboxylate MOF were successfully prepared by a modified solvothermal MOF-5 synthesis of Kaye and coworkers[34]. Like other MOFs, cubane-dicarboxylate based framework proved to be susceptible to polymorphism: slight variation of the conditions of preparation resulted in the formation of by-products. Here we focus on **1**, studies on related materials are in progress.

Equipments and materials. The solvothermal synthesis of the **1** were performed at elevated pressure and temperature in PTFE lined high-pressure vessels (PARR 4745 and PARR 4749). Heat treatments were carried out in an electric oven (Memmert UR30). Zinc nitrate hexahydrate (Sigma Aldrich, purum p.a. ≥ 99.0 %), cubane-1,4-dicarboxylic acid (Sigma Aldrich), dry N,N-dimethylformamide (Sigma Aldrich, anhydrous, 99.8 %), dry N-methyl-pyrrolidone (Sigma Aldrich, anhydrous, 99.5 %), toluene (VWR Chemicals, HiPerSolv CHROMANORM, ≥ 99.8 %) were used for the preparations without further purification. Chloroform (Sigma Aldrich, ACS reagent, ≥ 99.8 %) was dried with 3 Å molecular sieves. Prior to the experiments, the reaction vessels and the accessories were heat treated in a furnace at 200 °C overnight to remove adsorbed water. Weighing zinc nitrate hexahydrate and cubane-1,4-dicarboxylic acid was carried out under aerobic conditions as fast as possible. Great care was taken to avoid any uptake of moisture. Further manipulations of the materials, for example stirring solutions, settling and washing of the crystals were done under argon atmosphere, using either Schlenk technics or a glove box.

Preparation of 1. The solvothermal reactions were performed either in dimethylformamide (DMF) or in N-methyl-2-pyrrolidone (NMP) under argon atmosphere. Typically, the mixture of 179.5 mg (0.60 mmol) zinc nitrate hexahydrate and 38.2 mg (0.20 mmol) cubane-1,4-dicarboxylic acid was stirred in 20 ml of dry solvent for 30 minutes. The solution was filtered by a 0.2 μm PTFE membrane filter. Aliquots of 10 ml were closed into the high-pressure vessels and heated at 100 °C for 22 hours. After the reaction, the vessels were cooled down to room temperature in the furnace and the mixtures were stored under argon atmosphere. Transparent cubes of 100-200 μm sizes were formed, while the color of the solvent turned yellow. The possible by-products and the unreacted starting materials were removed by successive soaking in 5 ml of dry solvent for 3 times, 3 days each. The solvent was changed by decantation. For TG/MS studies, the crystals prepared in NMP solvent were used after rinsing them in acetone and dried in vacuum. In the crystals, used for X-ray diffraction, the original solvent was exchanged to toluene to prevent the diffusion of water into the cavities. For gas adsorption studies, we activated the crystals at ambient temperature by the exchange of the original solvents (DMF, NMP) to the low boiling point chloroform: the crystals were soaked in 5 ml of dry chloroform for 4 times, 1 days each.

Thermogravimetry/mass spectrometry (TG/MS). The TG/MS experiments were carried out in a modified Perkin Elmer TGS-2 thermobalance coupled to a Hiden HAL 301/PIC2 quadrupole mass spectrometer. The sample was measured in a platinum sample pan in argon and synthetic air atmospheres using 3.5 mg and 0.9 mg sample sizes, respectively. The thermobalance was purged by the carrier gas for 45 minutes using 140 ml min^{-1} flow rate before the experiments to remove the residual air from the furnace. The samples were heated up to 550 °C at a linear rate of 10 °C min^{-1} in inert and 5 °C min^{-1} in oxidative atmosphere. A portion of the volatile products

was introduced on-line into the mass spectrometer, where the product intensities were monitored using electron impact ionization (EI) with 70 eV electron energy. The mass range of m/z 14-130 was scanned excluding the ions of the argon carrier gas.

Single crystal X-ray diffraction. Single crystal X-ray diffraction measurements of the typically 100 μm size crystals were performed on an Agilent Supernova diffractometer equipped with dual microfocus source, kappa goniometer, position sensitive detector and dry nitrogen gas flow cooler. Data were taken at 100 K using the Cu source in a hemisphere of the reciprocal space up to 0.8 Å resolution. The diffraction power of the crystals was found to strongly depend on the preparation conditions and crystal selection. The data collection was controlled with the CrysAlis[35] software, while the structure solution and refinement were done with SHELX[36] software either called from scripts via the command line or from Olex2[37].

Conformation analysis. We calculated the total energy of several local conformations to determine the equilibrium geometry and the barriers of rotations. The studied fragments were terminated with H-atoms and the calculations were performed on these model molecules. The importance of weak nonbonded interactions made necessary the application of high-level quantum chemical methods. The B3LYP-gCP-D3/6-31G* approach was used [38-43] in the framework of ORCA package.

Porosity measurements.

We performed gas sorption experiments using Quantachrome Autosorb 1C static volumetric apparatus by measuring the increase of volume at equilibrium as a function of the relative pressure. All gases used were of 99.999% purity. All measurements were carried out at 77 K. The sample was outgassed prior to measurements at 393 K for 48 h. Adsorption data were

obtained using 0.013 g of sample and successive doses of the selected gas until $p/p_0 = 1$ relative pressure was reached.

RESULTS AND DISCUSSION

Formation of basic zinc cubane-1,4-dicarboxylate single crystals. To prepare high-quality single crystals of the cubane derivative, **1**, we optimized the experimental conditions, described in the previous paragraph. We applied two solvents, DMF and NMP, we changed the water content, the concentrations of Zn-nitrate, and cubane-dicarboxylate, the temperature and time of the reaction. The formed crystals were first investigated by optical microscopy and several samples of good shape and size were characterized by single crystal X-ray diffraction. Single-phase materials of cube-shaped transparent crystals proved to have the expected MOF structures. Only these samples were used for further experiments. In some cases, (*e.g.*, at higher Zn concentrations and/or at higher water contents) multiphase materials of cubes and needles were formed. The needles were Zn formate frameworks, as observed by other researchers previously[44].

Chemical composition, thermal stability and high-temperature activation. The chemical composition of the crystals can be determined by X-ray diffraction measurements, except the amount of the highly disordered solvent molecules inside the lattice. To determine the complete composition, thermogravimetry/mass spectrometry (TG/MS) studies were carried out. Besides the composition, TG/MS demonstrates the thermal stability and the release of the solvents, hereby revealing the necessary conditions of the thermal activation. The knowledge of the latter is essential for further host-guest applications. Fig. 1 shows the thermoanalytical results of **1**, *i.e.*, the TG/MS curves recorded during decomposition in an inert atmosphere (a) and the TG and

DTG curves measured in an oxidative atmosphere (b). In both cases, the starting material is the raw MOF (**1**), saturated with N-methyl-pyrrolidone (NMP) solvent. The characteristic decomposition step in the range of 100-200 °C corresponds to the release of NMP as the evolution profiles of the molecular ion (*m/z* 99) and other MS fragment ions indicate under inert conditions. The MS ion curves of NMP run parallel to the weight loss rate curve (DTG) without any detectable by-products. The profile of the ion at *m/z* 44 is somewhat complicated because it is a fragment ion of NMP at the lower temperature range, while at higher temperature it represents CO_2, a decomposition product of the carboxylate groups of the framework. Its minimum intensity at about 200 °C is accompanied with the formation of no other decomposition products showing that the total amount of the solvent is released, and the decomposition of the framework is still negligible, so the material is in activated state at 200 °C. The accompanied plateau of the mass indicates the possibility of reversible activation-filling processes. The decomposition of the framework increases gradually above the plateau and the maximum rate is at 450 °C. The most important volatile material detected by MS is CO_2, the decomposition product of carboxylate groups; however, small amount of benzene was also detected, which originates from the cubane segments. No mass loss can be observed above 500 °C. The residue is a black solid, obviously the mixture of ZnO and carbon. The latter is obviously the decomposition product of the cubylene units. The stoichiometry of this mixture is unknown, so it is not possible to determine its composition from this experiment.

To obtain a well-defined final product, we carried out a TG measurement in dry synthetic air (Fig. 1b). Under oxidative conditions, the decomposition of the framework is not separated well from the release of the solvent as shown by the significantly higher mass loss below 200 °C. On the other hand, the decomposition product of cubane burned out instead of carbonization. The

mass loss was finished at 450 °C, the residue was a white solid, pure ZnO. The composition of **1** was determined from the reductive and the oxidative thermoanalytical curves. The obtained stoichiometry is: $Zn_4O[C_8H_6(COO)_2]_3(C_5H_9NO)_6$.

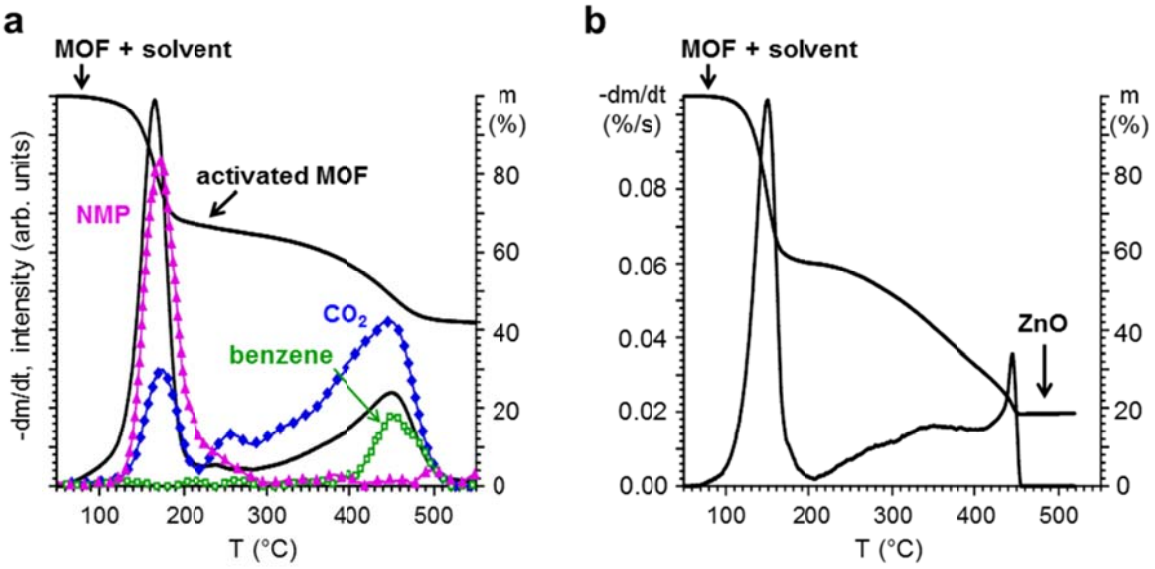

Figure 1. Thermal decomposition of **1** (a) in inert and (b) oxidative atmospheres. Solid lines: TG and DTG curves, ─▲─, NMP (*m/z* 99), ─◊─, CO_2 (*m/z* 44); ─□─, benzene (*m/z* 78);.

Crystal structure. The crystal structure of the new material, **1**, was determined by X-ray diffraction. As discussed above, the solvent of the crystals used for X-ray measurements was changed to toluene. The crystallographic data are given in Crystallographic Information Format (CIF) as Supplementary Material and summarized in Table 1.

Table 1. Crystallographic data of **1** (see also the supplementary CIF file)

Cubic lattice parameter:	12.77622(12) Å
Unit cell volume:	2085.49(6) $Å^3$
Temperature:	100 K
Space group:	$Pm\bar{3}m$
Sum formula with toluene solvent:	$C_{60}\ H_{72}\ O_{19}\ N_6\ Zn_4$
Radiation wavelength:	Cu K_α
Maximal Bragg-angle:	72.934°
Data completeness:	1.008
Number of reflections:	482
Number of parameters:	29
R-factor for all 482 observations:	0.0815
R-factor for 427 $F_o > 4\sigma(F_o)$ observations:	0.0755
Unit cell content, Wyckoff-positions and local point symmetry of fragments	
Origin choice: nodes at unit cell corners, linkers at cell edges	
One Zn_4O node tetrahedra disordered at	1 *a* $m\bar{3}m$ 000
Three OOC-C_8H_6-COO linkers disordered at	3 *d* 4/*mm.m* ½00, 0½0, 00½
Alternative origin choice: nodes at unit cell centers, linkers at center-center lines	
One Zn_4O node tetrahedra disordered at	1 *b* $m\bar{3}m$ ½½½
Three OOC-C_8H_6-COO linkers disordered at	3 *c* 4/*mm.m* 0½½, ½0½, ½½0

The reflections are indexed with a cubic lattice of $a = 12.776$ Å. The histogram of the projections of unindexed peaks onto the crystallographic axes and the computational reconstruction of the main reciprocal planes show no superreflections, thus exclude larger unit cells. Missing extinctions indicate the absence of lattice centering, screw axes and glide planes. The analysis of intensity distributions suggests $m3,\bar{m}$ Laue symmetry with $R_{sym} = 0.051$ and $R_{merge} = 0.050$. Three space groups correspond to the above conditions: $P432$, $P4,\bar{3}m$ and $Pm3,\bar{m}$. The attempt to solve the structure in all these space groups results in identical structures. The only difference is the larger number of independent atoms, hence more degrees of freedom and insignificantly better refinement indicators in the lower symmetry space groups. Also, the Flack-parameter is close to 0.5 for the two lower-symmetry, non-centrosymmetric groups indicating the presence of inversion symmetry. Therefore, we concluded that the space group is $Pm3,\bar{m}$. The structure can be explored via the Supplementary CIF file.

Based on the knowledge of the structural components and their refined occupancies, the structure is heavily disordered; a common characteristics of non-activated MOF structures[45]. Various disordered parts of the structure are handled as follows:

(*i.*) The tetrahedral ($T_d = 4,\bar{3}m$) Zn_4O units at the 1*a* 000 (or equivalently the 1*b* ½½½) Wyckoff positions yield an average octahedral $O_h = m3,\bar{m}$ symmetry, *i.e.,* a twofold disorder of equal probability. This disorder cannot be dynamic, and its randomness is fixed during the crystal growth.

(*ii.*) The not fully compatible molecular symmetry of the rigid cubylene linker ($D_{3d} = 3,\bar{m}$) and the 3*d* ½00 (or equivalently the 3*c* 0½½) positions of $D_{4h} = 4/mmm$ symmetry (where the center of linkers is located) are reconciled by finding their common subgroup of the largest order, which is $C_{2h} = 2/m$ and can possess three distinct orientations. Because of the carboxylate

links, the primary axis of this subgroup cannot coincide with the linker axis but must be perpendicular to it and set at 0° or 45° relative to one of the appropriate unit cell directions. Placing two rigid cubylene units ($d_{C\text{-}C}$ = 1.575 Å, $d_{C\text{-}H}$ = 1.075 Å) according to the subgroups orientations, the point symmetry generates 24 equidistant off-axial carbon positions, resulting in two toroidal electron density rings. This well approximates a uniaxial rotation of the cubylene unit, which is the physical model behind this description. Further developing this idea, the anisotropic thermal displacement factors of these off axial atoms are restricted by a (TLS-like) rigid model, allowing simple libration about the linker axis.

(*iii.*) Taken into account the disordered framework, about 62.5% of the unit cell volume is accessible for solvent molecules due to the holes between adjacent cavities. These are filled with toluene in the crystals prepared for X-ray diffraction measurements. The atomic positions for these disordered molecules could not be determined, therefore we searched for an optimal placement of a whole rigid toluene molecule and let the space group symmetries to multiply this molecule and fill the void according to the observed low electron density. Technically this was performed with a simulated annealing optimization procedure. The large error of positions and the large displacement factors result in a blurred, not localized electron density. The resulting occupancies indicate 8.06 toluenes per unit cell, *i.e.*, all corners of the cubic void contain a solvent molecule that is also a plausible result based on volume considerations.

This structure results in $R = 0.0815$ for all 482 observations and $R = 0.0755$ for 427 $F_o > 4\sigma(F_o)$ with 29 refined parameters and 0 restraints. See table 1 and the Supplied CIF file for more details. A perspective space fill view of the average structure of basic zinc cubane-1,4-dicarboxylate, **1**, is displayed in Fig.2; H-atoms are omitted for clarity.

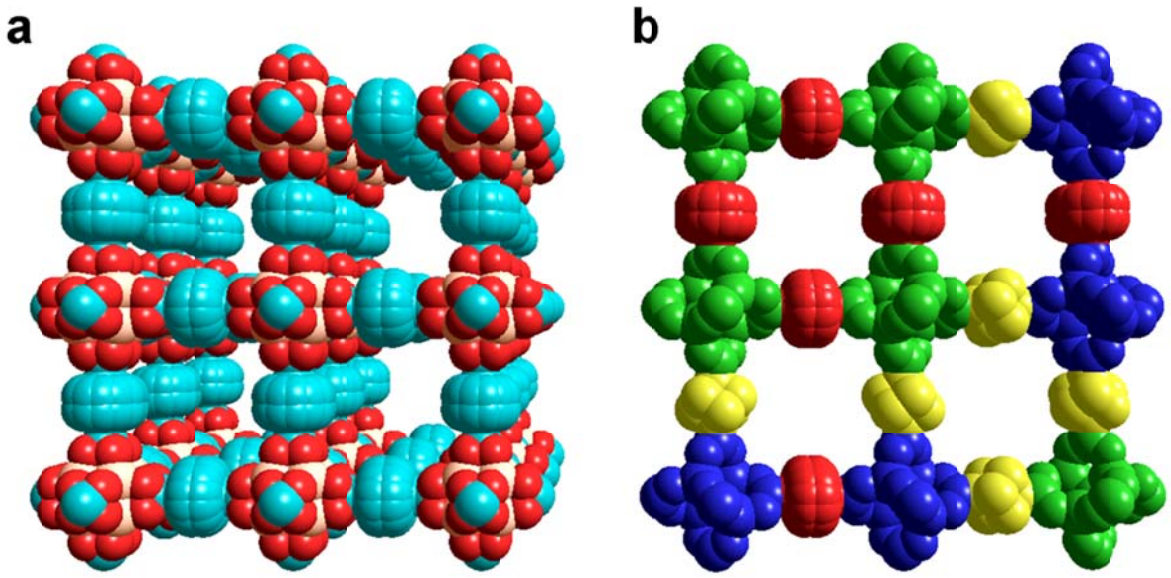

Figure 2. Perspective view of the crystal lattice of basic zinc cubane-1,4-dicarboxylate, **1**. a: Average structure, corresponding to the $Pm\bar{3}m$ space group. b: A snapshot of the (001) plane between the temperatures of the predicted 2-step freezing of the spacers. An orientational glass of two perpendicular SBUs (green and blue) are connected with static (yellow) and rotating (red) cubylene units.

Conformation and dynamics. To explain the structural characteristics, it is instructive to compare the molecular and supramolecular interactions of **1** with those of the closely related structures of basic zinc acetylene-dicarboxylate[46] and basic zinc benzene-1,4-dicarboxylate[6]. The *pcu* topology of the basic zinc cubane-1,4-dicarboxylate framework (**1**) is the same as in IRMOF-0 and MOF-5; however, the space groups and sizes of the unit cells are different. The differences can be explained in terms of the molecular interactions between the spacers and the adjacent SBUs as well as the supramolecular spacer-SBU and SBU-SBU interactions. Fig. 3 compares the possible geometries of the SBU-spacer-SBU fragments, which are predominantly responsible for the crystal structures. These fragments were terminated with H-atoms and the

conformational energies of the model compounds were calculated. IRMOF-0 represents the simplest case: the orientation of the two SBUs is the same, resulting in a D_{2d} *(=222)* local symmetry of the fragment (Fig. 3a). Supporting the previous experimental result[s47], our B3LYP-gCP-D3/6-31G(d) calculation shows that the energy of this conformation is 4.07 kJ/mol lower, than the other possible conformation of two perpendicular SBUs with D_{2h} *(=2/mmm)* symmetry. Since the cylindrical -C≡C- spacer has no influence on the orientation, the electrostatic repulsion of the carboxylic O-atoms may control the equilibrium conformation. The case of MOF-5 is just the opposite: the terephthalate unit is coplanar because of the conjugated π-electron system, enforcing the D_{2h} *(=2/mmm)* symmetry to the fragment (Fig. 3 d). In a hypothetic conformation of D_{2d} symmetry the conjugation would be broken. Its calculated energy of formation is 29.6 kJ/mol higher than that of the D_{2h} symmetry, excluding the possibility of D_{2d} conformations in MOF-5. The high differences in the energies of the conformations support the experimental results that both IRMOF-0 and MOF-5 form highly ordered crystals. The significant disorder, observed in the cubane-1,4-dicarboxylate derivative can be attributed to the flexibility of the axial σ-bonds and the different local symmetry of the spacer and the SBU-SBU pairs. Because in the precursor dicarboxylate the orientations of the two carboxylic groups and the central cubylene fragment are independent of each other, the local symmetry of the SBU-SBU pairs in the crystal can be either D_{2d} (Fig. 3b and c) like in IRMOF-0 or D_{2h} (Fig. 3e and f) like in MOF-5. In the fragments of Fig. 3b and e the orientation of the cubylene unit can be characterized by the torsion angle ϕ_{OCCC} determined by the atoms: O(carboxylic)-C(carboxylic)-C(cubylene axial)-C(cubylene lateral). The combination of the D_{3d} symmetry of cubylene with the D_{2d} symmetry SBU pairs decreases the symmetry of the fragment (Fig. 3b and e). The resultant point group is C_1 in general case, C_{1h} at $\phi_{OCCC} = 0° \pm k\times30°$ and C_2 at $\phi_{OCCC} = 15° \pm k\times30°$ where k is

integer. Similarly, the D_{3d} - D_{2h} combination results in C_i, D_2, and C_{2h} point groups in the same ranges of ϕ_{OCCC}. The calculations discussed below show that the higher symmetry conformations are unstable; they correspond to the local maxima of the conformational energies (Fig. 4a and b). The conformations displayed, correspond to the minimal energies at ϕ_{OCCC} = 25° in both cases. However, these conformations are not consistent with ordered cubic structures, so the orientations of cubylene units are multiplied, resulting in disorder. Considering the energy minima in Fig. 4a and b, 8 superimposed orientations at ϕ_{OCCC} = ±5°+k×30° (k=0, 1, 2, 3) reconstruct the D_{2d} symmetry fragment of Fig. 3c, and 4 superimposed orientations at ϕ_{OCCC} = 30°± 5°+k×60° (k=0, 1) that of the D_{2h} symmetry (Fig. 3f). The former could form a crystal with $P4,\bar{3}m$ space group, while the latter with $Fm3,\bar{m}$ space group. The D_{2d} symmetry fragment is a little more stable, but the difference of calculated energy, 0.41 kJ/mol, is too low. Thus, both local structures contribute to the experimentally observed $Pm3,\bar{m}$ space group resulting in the average fragments of D_{4h} symmetry (Fig. 3g).

The distinct conformations of the cubylene units discussed above can be only realized at very low temperatures. For the fragment of D_{2d} symmetry SBU pairs, the value of the barrier is 0.06 kJ/mol, while that for the D_{2d} symmetry is 0.11 kJ/mol. These unusually low barriers can be attributed to characteristic distances of the interacting nonbonded pairs of atoms and the local symmetry of the fragment. The leading terms in the conformational energy are the nonbonded interactions between the carboxylic O-atoms and the lateral C-atoms of the cubylene unit. The shortest nonbonded C---O distances vary between 3.03-3.89 Å *i.e.* from slightly repulsive to attractive ranges. All the other nonbonded interactions are attractive, so even the sum of these terms would be small. However, the combination of the threefold axial symmetry of C-atoms with the twofold symmetry of the O-atoms cancels out the dependence of the predominant

portions of the interactions: while the distance of some interacting pairs increases, the distance of other corresponding pairs decreases, resulting in the rather complex shapes and low amplitudes of the conformational energy diagrams of Fig. 4 a and b. The low energy barriers suggest free uniaxial rotation of the cubylenes at ambient conditions. Upon cooling to low temperatures, first the rotation of the D_{2h} symmetry fragment freezes out, then the other of D_{2d} symmetry. The uniaxial rotation of the cubylenes has no influence on the length of the edge, *i.e.*, the cubic cell parameter. The rigid cell and the free rotation together satisfy the conditions of robust dynamic, described previously[1]. In this system, the SBUs and the connecting axial C-C bonds represent the stators, while the cubylenes the rotors. The rotation, facilitated by the cancelled nonbonded interactions, resembles the so-called molecular bearing effect, observed previously in the supramolecular rotor-stator crystals of fullerene-cubane system[28] where the incommensurable arrangement of the atoms in the matching surfaces enhanced the rotation. On the other hand, the predicted dynamics of **1** is significantly different from that of MOF-5. For comparison, we also calculated the conformational energy of the SBU-spacer-SBU fragment of MOF-5. As shown in Fig. 4c, the barrier of the rotation of the p-phenylene unit is 74.9 kJ/mol. This value is consistent with previous calculations and NMR experiments[23], indicating that only jump rotation of the p-phenylene units is possible at elevated temperatures. The rotation barrier of the hypothetic fragment with D_{2d} symmetry SBUs would be much easier; however, the equilibrium energy of this fragment is too high to be considered.

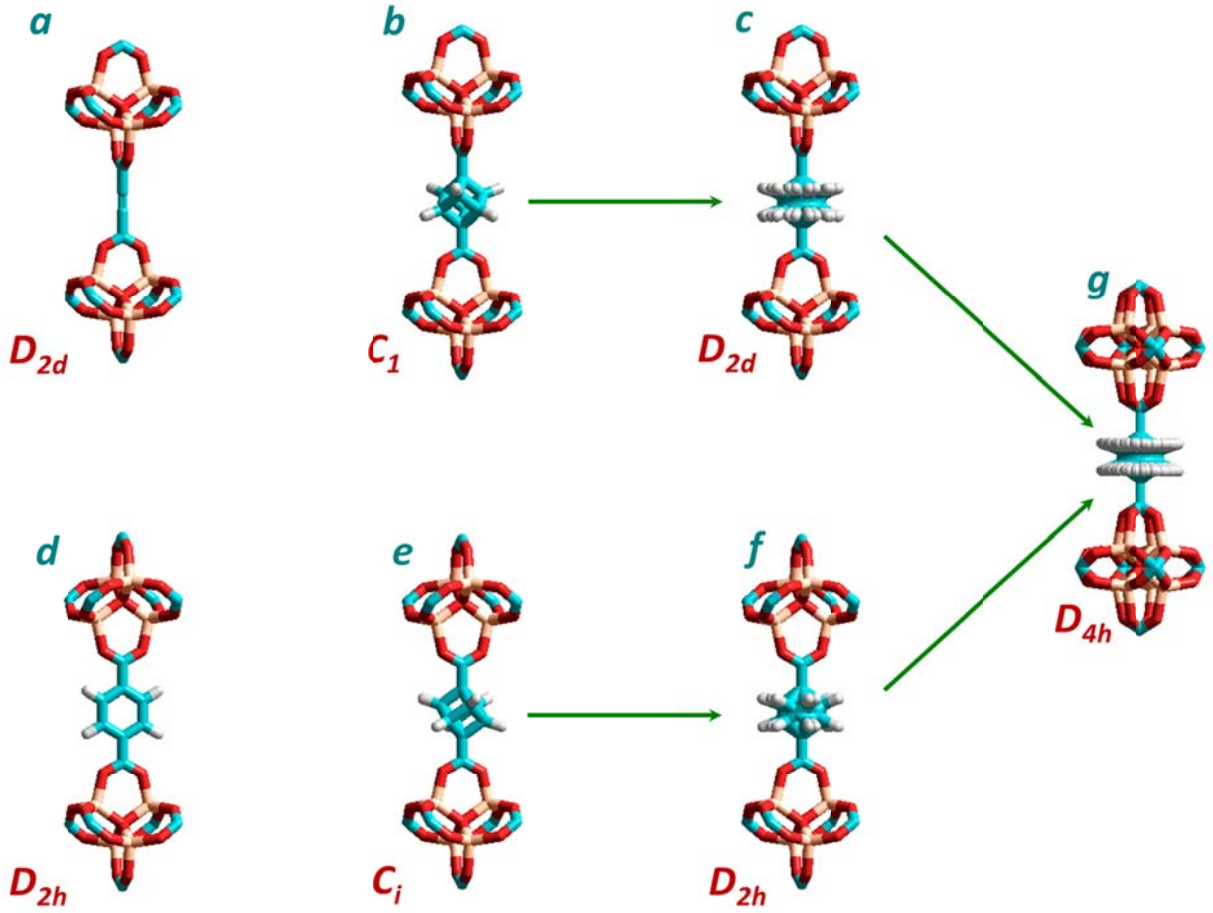

Figure. 3. Local conformations of the SBU-spacer-SBU fragments in IRMOF-0 (a), in MOF-5 (d), and in the cubane-dicarboxylate framework, **1,** (b, c, e, f, g), illustrating the derivation of the average conformation of **1**.

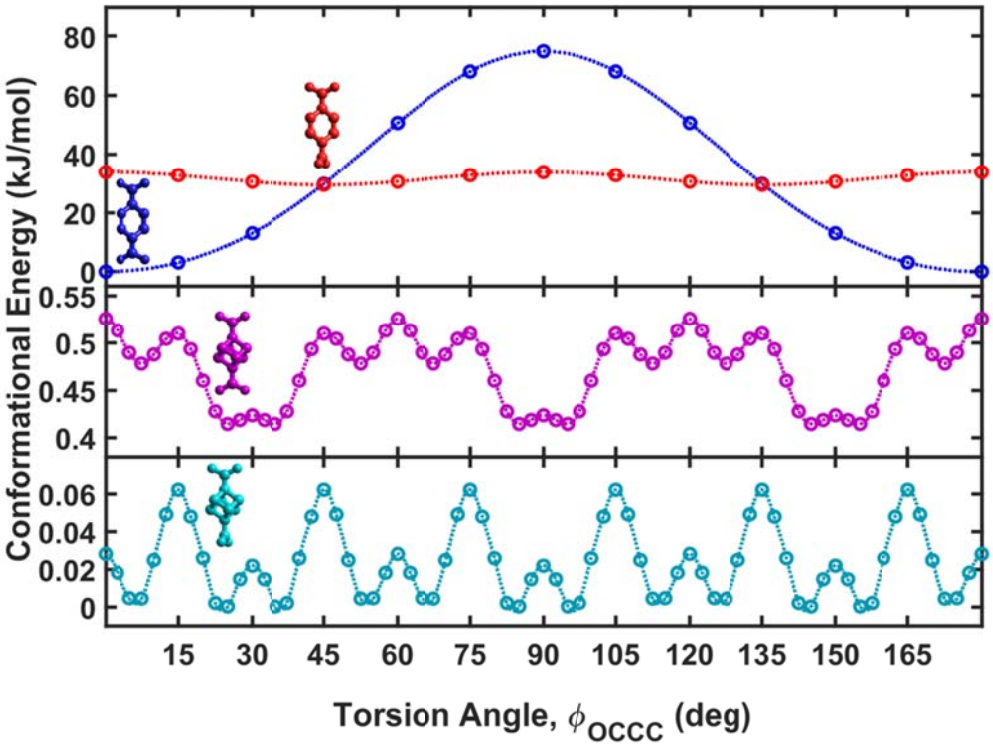

Figure 4. Calculated conformational energy of various fragments of basic Zn-1,4-dicarboxylate and MOF-5. a: D_{2d} -dicarboxylate of **1**, b: D_{2h} -dicarboxylate of **1**, c: blue: D_{2h}-dicarboxylate of MOF-5, red: hypothetic D_{2d}-dicarboxylate of MOF-5.

Adsorption-desorption of inert gases. Nitrogen and argon adsorption-desorption isotherms are of type I according to the IUPAC classification which is characteristic for microporous material. The isotherms rise sharply at low relative pressure where micropore (of width <2 nm) filling occurs in the precapillary condensation range. Even though the obtained isotherm is similar to Langmuir one the Langmuir equation is not suitable for determination of specific surface area for several reasons[47]. Instead BET surface analyses have been performed for determination of specific surface area using the relative pressure range of 0.000005-0.05 in the

nitrogen adsorption isotherm as a range of linearity (using a molecular cross-sectional area for N_2 of 0.162 nm^2). The BET method also has some weaknesses in case of microporous materials since it has several assumptions which do not hold[48]. One assumption is that a monolayer forms on the pore walls but in case of microporous material it is quite difficult to distinguish micropore filling, which occurs at relative pressure below 0.15 from that of the monolayer formation process. To find the linear BET range the BET equation must be limited to the range where plots of Vx(1-p/p_0) continuously increasing in the function of p/p_0.

The pore size distribution was calculated both by HK (Horvath-Kawazoe) and SF (Saito-Foley) methods, which are suitable for microporous materials. The HK method is adequate rather carbon materials with slit-like pores but SF which is developed from HK, convenient for micropores with different shapes[49]. In our case both methods gave similar results. Microporosity measurements were performed using both nitrogen and argon. Although nitrogen is the most commonly used adsorptive to determine porosity, but due to its quadrupole moment in certain cases argon could give more reliable results[50] for quantitative evaluation of the microporosity especially in the ultramicropore (of width<0.7 nm) range. Since the SBUs contain Zn ion and various polar groups argon isotherm was also measured to eliminate the possibility of false result due to N_2 quadrupole moment[51].

According to ideal gas law, **1** has 1.52 wt. % gravimetric H_2 uptake at 77 K and 1 atm, which is somewhat higher, than the low pressure H_2 uptake for MOF-5 (1.32 wt. %)[52]. Furthermore, **1** has significantly higher volumetric hydrogen uptake (10.4 g/l), than that of MOF-5 (7.9 g/l)[53], which is the consequence of higher density ($d_{single\text{-}crystal}$=0.68 gcm^{-3}) and higher gravimetric uptake of basic zinc cubane-1,4-dicarboxylate framework (**1**).

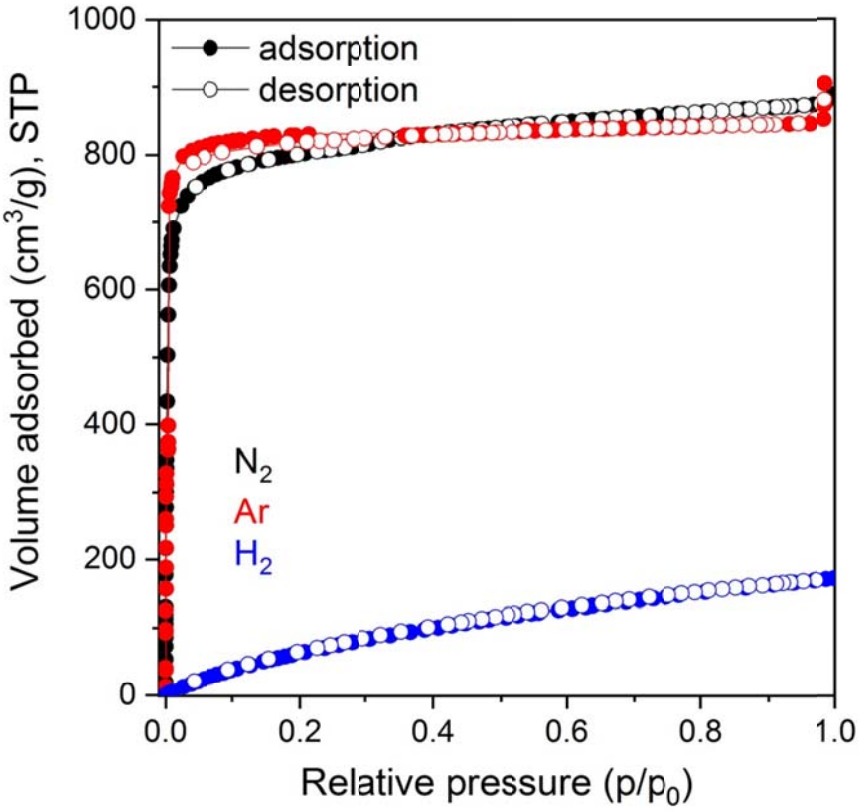

Figure 5. Adsorption isotherms of basic zinc cubane-dicarboxylate, **1**.

CONCLUSIONS

In summary, we prepared a new MOF structure **1**, consisting of basic Zn cubane-1,4-dicarboxylate fragments. The chemical composition of the pristine material is $Zn_4O[C_8H_6(CO_2)_2]_3Sol_n$ where Sol is DMF or NMP. The solvent molecules can be removed by a heat treatment in inert atmosphere or in vacuum at 200 °C or exchanged for more volatile chloroform by rinsing at ambient temperature. The topology of **1** is a primitive cubic framework of basic Zn-carboxylate nodes and 1,4-cubylene spacers. The constitution is closely related to MOF-5, because of the same SBUs, the similar sizes of the organic linkers and the same underlying topologies. On the other hand, the chemical differences of the conjugated π-electron

system of terephthalate and the σ-bonded cubane-1,4-dicarboxylate ions result in significant differences in the conformations: while terephthalate is a planar molecule of rigid bonds, **1** is more flexible, the 1,4-cubylene spacers are orientationally disordered, they probably rotate about their main axis, *i.e.*, about the node-node axes. The $Pm\bar{3}m$ space group of **1** has higher symmetry than the constituent fragments so the disordered structure is the average of several lower symmetry unit cells. The O_h symmetry vertices of the framework can be considered as the average of two randomly distributed perpendicular SBUs of T_d symmetry. The site symmetry of the linker centers is D_{4h}, the corresponding average structure consists of at least four or eight D_{3d} symmetry cubylenes, depending on the orientations of the adjacent SBUs. Due to the high number of equivalent conformations, the average structure can be described in terms of a random distribution of axially disordered cubylenes. The weak interactions make possible the rotation of cubylenes; however, the dynamics depends on the local conformations of the two carboxylic groups. Symmetry considerations show that the interactions with SBU pairs of D_{2d} symmetry are almost independent on the orientation of the central cubylene, allowing free rotation even at low temperature. The barrier of the rotation between SBU pairs of D_{2h} symmetry is about 8 kJ/mol. It is nine times lower than the barrier of the p-phenylene rotation in MOF5 so this group of cubylenes can freely rotate at ambient conditions and at moderately low temperatures. Future solid-state NMR and IR-spectroscopic experiments are needed to justify our prediction for this 2-step phase transition and to reveal the quantitative characteristics of this complex dynamics.

ASSOCIATED CONTENT

Supporting Information

The following files are available free of charge. Crystallographic information file for **1** (CIF) and checkcif report (PDF).

AUTHOR INFORMATION

Corresponding Author

*E-mail: kovats.eva@wigner.mta.hu

ORCID: Éva Kováts: 0000-0002-8358-857X

ACKNOWLEDGMENT

The research was supported by the National Research, Development and Innovation Office (NKFIH) through projects FK-125063, OTKA NK105691 and VEKOP-2.3.3-15-2016-00001.

REFERENCES

1. Deng, H.; Olson, M. A.; Stoddart, J. F.; and Yaghi O. M. Robust Dynamics. *Nature Chemistry* **2010**, 2, 439–443.

2. Furukawa, H.; Cordova, K. E.; O'Keeffe, M.; Yaghi, O. M. The Chemistry and Applications of Metal-Organic Frameworks. *Science* **2013**, 341 (6149), 1-12.

3. Batten, S. R.; Champness, N. R.; Chen, X.-M.; Garcia-Martinez, J.; Kitagawa, S.; Öhrström, L.; O'Keeffe, M.; Suh, M. P.; Reedijk, J. Coordination Polymers, Metal-Organic Frameworks and the Need for Terminology Guidelines. *Cryst. Eng. Comm.* **2012**, 14, 3001-3004.

4. Fujita, M.; Kwon, Y. J.; Washizu, S.; Ogura, K. Preparation, Clathration Ability, and Catalysis of a Two-Dimensional Square Network Material Composed of Cadmium(II) and 4,4'-Bipyridine. *J. Am. Chem. Soc.* **1994**, 116, 1151–1152

5. Li, H.; Eddaoudi, M.; Groy, T. L. and Yaghi, O. M. Establishing Microporosity in Open Metal−Organic Frameworks: Gas Sorption Isotherms for Zn(BDC) (BDC = 1,4-Benzenedicarboxylate). *J. Am. Chem. Soc*. **1998**, 120, 8571-8572

6. Li, H.; Eddaoudi, M.; O'Keeffe, M.; Yaghi, O. M. Design and Synthesis of an Exceptionally Stable and Highly Porous Metal-Organic Framework. *Nature* **1999**, 402, 276-279.

7. Eddaoudi,M.; Kim, J.; Rosi, N.; Vodak, D.; Wachter, J.; O'Keeffe, M.; Yaghi, O. M. Systematic Design of Pore Size and Functionality in Isoreticular MOFs and Their Application in Methane Storage. *Science* **2002**, 295, 469-472.

8. Czaja, A. U.; Trukhanb, N. and Müller, U. Industrial Applications of Metal-Organic Frameworks. *Chem. Soc. Rev.* **2009**, 38, 1284–1293.

9. Mueller, U.; Schubert, M.; Teich, F.; Puetter, H.; Schierle-Arndt, K. and Pastre, J. Metal–Organic Frameworks—Prospective Industrial Applications. *J. Mater. Chem.* **2006**, 16, 626–636.

10. Hayashi, H.; Coté, A. P.; Furukawa, H.; O'Keeffe, M. and Yaghi, O. M. Zeolite A Imidazolate Frameworks, *Nat. Mater.* **2007**, 6, 501-506.

11. Stock, N. and Biswas, S. Synthesis of Metal-Organic Frameworks (MOFs): Routes to Various MOF Topologies, Morphologies, and Composites, *Chem. Rev.* **2012,** 112, 933-969.

12. Yoshizawa, M.; Klosterman, J. K.; and Fujita, M. Functional Molecular Flasks: New Properties and Reactions within Discrete, Self-Assembled Hosts, *Angew. Chem. Int. Ed.* **2009**, 48, 3418–3438.

13. Li, J.-R.; Kuppler, R. J. and Zhou, H.-C. Selective Gas Adsorption and Separation in Metal-Organic Frameworks. *Chem. Soc. Rev.* **2009**, 38, 1477–1504.

14. Han, S. S.; Mendoza-Cortés, J. L.; and Goddard III, W. A; Recent Advances on Simulation and Theory of Hydrogen Storage in Metal–Organic Frameworks and Covalent Organic Frameworks. *Chem. Soc. Rev.* **2009**, 38, 1460–1476.

15. Murray, L. J.; Dinca, M. and Long, J. R. Hydrogene Storage in Metal-Organic Frameworks. *Chem. Soc. Rev.* **2009**, 38, 1294–1314.

16. Skarmoutsos, I.; Eddaoudi, M.; Maurin, G. Peculiar Molecular Shape and Size Dependence of the Dynamics of Fluids Confined in a Small-Pore Metal–Organic Framework. *J. Phys. Chem. Lett.* **2018**, 9, 3014−3020

17. Uemura, T.; Yanaia, N. and Kitagawa, S. Polymerization Reactions in Porous Coordination Polymers. *Chem. Soc. Rev.* **2009**, 38, 1228–1236.

18. Ma, L.; Abney, C. and Lin, W. Enantioselective Catalysis with Homochiral Metal-Organic Frameworks. *Chem. Soc. Rev.* **2009**, 38, 1248–1256 .

19. Wang, Z. and Cohen, S. M. Postsynthetic Modification of Metal-Organic Frameworks. *Chem. Soc. Rev.* **2009**, 38, 1315–1329.

20. Allendorf, M. D.; Bauer, C. A.; Bhakta, R. K.; Houk, R. J. T. Luminescent Metal-Organic Frameworks. *Chem. Soc. Rev.* **2009**, 38, 1330–1352.

21. Kurmoo, M. Magnetic Metal-Organic Frameworks. *Chem. Soc. Rev.* **2009**, 38, 1353–1379.

22. Ryder, M. R.; Zeng, Z.; Titov, K.; Sun, Y.; Mahdi, E. M.; Flyagina, I.; Bennett, T. D.; Civalleri, B.; Kelley, C. S.; Frogley, M. D.; Cinque, G. and Tan, J. –C. Dielectric Properties of Zeolitic Imidazolate Frameworks in the Broad-Band Infrared Regime. *J. Phys. Chem. Lett.* **2018**, 9 (10), 2678−2684

23. Gould, S. L.; Tranchemontagne, D.; Yaghi, O. M. and Garcia-Garibay, M. A. Amphidynamic Character of Crystalline MOF-5: Rotational Dynamics of Terephthalate Phenylenes in a Free-Volume, Sterically Unhindered Environment. *J. Am. Chem. Soc.* **2008**, 130, 3246–3247.

24. Khudozhitkov, A. E.; Kolokolov, D. I. and Stepanov, A. G. Characterization of Fast Restricted Librations of Terephthalate Linkers in MOF UiO-66(Zr) by ^{2}H NMR Spin–Lattice Relaxation Analysis. *J. Phys. Chem. C*, **2018**, 122 (24), 12956-12962.

25. Farha, O. K.; Yazaydın, A. Ö.; Eryazici, I.; Malliakas, C. D.; Hauser, B. G.; Kanatzidis, M. G.; Nguyen, S. T.; Snurr, R. Q. De Novo Synthesis of a Metal–Organic Framework Material Featuring Ultrahigh Surface Area and Gas Storage Capacities. *Nat. Chem.* **2010**, 2, 944-948.

26. Farha, O. K.; Eryazici, I.; Jeong, N. C.; Hauser, B. G.; Wilmer, C. E.; Sarjeant, A. A.; Snurr, R. Q.; Nguyen, S. T.; Yazaydın, A. Ö. and Hupp, J. T. Metal–Organic Framework Materials with Ultrahigh Surface Areas: Is the Sky the Limit? *J. Am. Chem. Soc.* **2012**, 134 (36), 15016-15021.

27. Vogelsberg, C. S. and Garcia-Garibay, M.A. Crystalline molecular machines: function, phase order, dimensionality, and composition. *Chem. Soc. Rev*. **2011**, 41, 1892-1910.

28. Pekker, S.; Kováts, É.; Oszlányi, G.; Bényei, Gy.; Klupp, G.; Bortel, G.; Jalsovszky, I.; Jakab, E.; Borondics, F.; Kamarás, K.; Bokor, M.; Kriza, G.; Tompa, K.; Faigel, G. Rotor-stator molecular crystals of fullerenes with cubane, *Nat. Mater.* **2005**, 4, 764-767.

29. Li, Q.; Zhang, W.; Milanjic, O. S.; Sue, C.–H.; Zhao, Y.-L.; Liu, L.; Knobler, C. B.; Stoddart, J. F.; Yaghi, O. M. Docking in Metal-Organic Frameworks. *Science*, **2009**, 325, 855-859.

30. Sue, A. C.-H; Mannige, R. V.; Deng, H.; Cao, D.; Wang, C.; Gandara, F.; Stoddart, J. F.; Whitelam, S.; Yaghi, O. M. Heterogeneity of Functional Groups in a Metal–Organic Framework Displays Magic Number Ratios. *Proc. Nat. Acad. Sci. USA*, **2015**, 112, 5591-5596.

31. Tranchemontagne, D. J.; Mendoza-Corte´s, J. L.; O'Keeffe, M.; Yaghi, O. M. Secondary Building Units, Nets and Bonding in the Chemistry of Metal-Organic Frameworks. *Chem. Soc. Rev.* **2009,** 38, 1257–1283.

32. Eddaoudi, M.; Kim, J.; Vodak, D.; Sudik, A.; Wachter, J.; O'Keeffe, M. and Yaghi, O. M. Geometric Requirements and Examples of Important Structures in the Assembly of Square Building Blocks. *Proc. Nat. Acad. Sci.*, **2002**, 99, 4900-4904.

33. Cotton, F. A.; Daniels, L. M.; Lin, C.; Murillo, C. A.; Yu, S-Y. Supramolecular Squares with Rh_2^{4+} Corners. *J. Chem. Soc. ,Dalton Trans.*, **2001**, 0, 502-504.

34. Kaye, S. S.; Dailly, A.; Yaghi, O. M. and Long, J. R. Impact of Preparation and Handling on the Hydrogen Storage Properties of Zn_4O(1,4-benzenedicarboxylate)$_3$ (MOF-5). *J. Am. Chem. Soc*., **2007**, 129, 14176-14177.

35. CrysAlisPRO, Oxford Diffraction /Agilent Technologies UK Ltd, Yarnton, England

36. Sheldrick, G. M. A Short Hystory of SHELX. *Acta Crystallogr. A.* 2008 ;64 (Pt 1),112-122.

37. Dolomanov, O. V.; Bourhis, L. J.; Gildea, R. J.; Howard, J. A. K.; Puschmann, H. OLEX2: a Complete Structure Solution, Refinement and Analysis Program. *J. Appl. Cryst*. **2009**, 42, 339-341.

38. Kruse, H.; Goerigk, L.; Grimme, S. Why the Standard B3LYP/6-31G* Model Chemistry Should Not Be Used in DFT Calculations of Molecular Thermochemistry: Understanding and Correcting the Problem. *J. Org. Chem.* **2012**, 77, 10824-10834.

39. Kruse, H.; Grimme, S. A Geometrical Correction for the Inter- and Intra-molecular Basis Set Superposition Error in Hartree-Fock and Density Functional Theory Calculations for Large Systems. *J. Chem. Phys.*, **2012**, 136, 154101.

40. Grimme, S.; Ehrlich, S.; Goerigk, L. Effect of the damping function in dispersion corrected density functional theory. *J. Comput. Chem.* **2011**, 32, 1456–1465.

41. Grimme, S.; Antony, J.; Ehrlich, S. and Krieg, H. A Consistent and Accurate Ab Initio Parametrization of Density Functional Dispersion Correction (DFT-D) for the 94Eelements H-Pu. *J. Chem. Phys.* **2010**, 132, 154104.

42. Hehre, W. J.; Ditchfield, R. and Pople, J. A. Self—Consistent Molecular Orbital Methods. XII. Further Extensions of Gaussian—Type Basis Sets for Use in Molecular Orbital Studies of Organic Molecules. *J. Chem. Phys.* **1972**, 56, 2257-2261.

43. V. A. Rassolov, J. A. Pople, M. A. Ratner, and T. L. Windus, 6-31G* Basis Set for Atoms K Through Zn. *J. Chem. Phys*. **1998**, 109, 1223-1229.

44. Clausen, H. F.; Poulsen, R. D.; Bond, A. D.; Chevallier, M.-A. S.; Iversen, B. B. Solvothermal Synthesis of New Metal Organic Framework Structures in the Zinc–Terephthalic Acid–Dimethyl Formamide System. *J. Solid State Chem.*, *2005*, 178, 3342-3351.

45. Gándara, F. and Bennett, T. D. Crystallography of Metal–Organic Frameworks, *IUCrJ* **2014**, 1, 563–570.

46. Trachemontagne, D. J.; Hunt, J. R.; Yaghi, O. M.; Room temperature synthesis of metal-organic frameworks: MOF-5, MOF-74, MOF-177, MOF-199, and IRMOF-0. *Tetrahedron*, **2008**, 64 (36), 8553-8557.

47 34. Rouquerol, J.; Llewellyn, P.; Rouquerol, F. Is the BET equation applicable to microporous adsorbents? *Studies in Surface Science and Catalysis*, 2007, 160, pp 49-56.

48 35. Walton, K. S.; Snurr, R.Q. Applicability of the BET Method for Determining Surface Areas of Microporous Metal-Organic Frameworks. *J. Am. Chem. Soc.*, **2007**, 129, 8552-8556.

49 36. Groen, J. C.; Peffer, L. A. A.; Pérez-Ramírez, J. Pore Size Determination in Modified Micro- and Mesoporous Materials. Pitfalls and Limitations in Gas Adsorption Data Analysis. *Micropor. Mesopor. Mat.*, **2003**, 60, 1-17.

50 37. Thommes, M. Physical Adsorption Characterization of Nanoporous Materials. *Chemie Ingenieur Technik*, **2010**, 82 (7) 1059-1073.

51. Rouquerol, F.; Rouquerol, J.; Sing, K. S. W.; Llewellyn, P.; Maurin, G. *Adsorption by Powders and Porous Solids: Principles, Methodology and Applications*, Academic Press: Oxford, U.K., 2014

52. Rowsell, J. L. C.; Milward, A. R.; Park, K. S. and Yaghi, O. M. Hydrogen Sorption in Functionalized Metal−Organic Frameworks. *J. Am. Chem. Soc*., **2004**, 126, 5666-5667.

53. Kim, H.; Das, S.; Kim, M. G.; Dybtsev, D. N.; Kim, Y. and Kim, K. Synthesis of Phase-Pure Interpenetrated MOF-5 and Its Gas Sorption Properties. *Inorg. Chem.,* 2011, 50, 3691-3696.

FOR TABLE OF CONTENTS ONLY

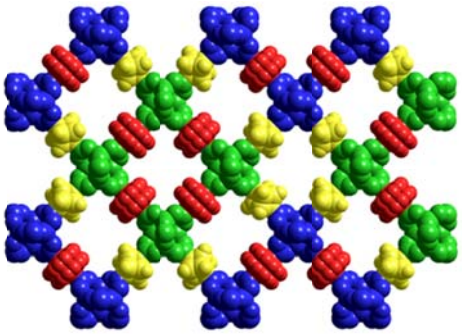

SYNOPSIS

By replacing a benzene ring with a cubane cage, a new high-symmetry MOF was synthetized with similar lattice parameters and promising supramolecular properties. The dynamics of the new material is unique: the stable frame contains uniaxial rotating edges representing so-called robust dynamics.